Widespread nociceptive maps in the human neonatal somatosensory cortex.

Laura Jones[1†], Madeleine Verriotis*, Robert J. Cooper[2], Maria Pureza Laudiano-Dray[1], Mohammed Rupawala[1], Judith Meek[3], Lorenzo Fabrizi[1], & Maria Fitzgerald[1]

[1] Department of Neuroscience, Physiology & Pharmacology, University College London, London, WC1E 6BT, UK
[2] DOT-HUB, Department of Medical Physics & Biomedical Engineering, University College London, London, WC1E 6BT, UK
[3] Elizabeth Garrett Anderson Obstetric Wing, University College London Hospitals, London, WC1E 6DB, UK

[*]**Current address**: Department of Developmental Neuroscience, University College London Great Ormond Street Institute of Child Health, London, WC1N 1EH, UK

[†] **Corresponding Authors**: m.fitzgerald@ucl.ac.uk and laura.jones@ucl.ac.uk

Running title: Touch & pain topography in the human infant cortex
No. of Pages: 22
No. of Figures: 4
No. of Tables: 1
No. of words Abstract: 250
No. of words Introduction: 592
No. of words Discussion: 1500

Conflict of interest statement: RJC holds financial interests in Gowerlabs Ltd, who produce the device used in this study. The authors declare no other conflict of interest in this study.

Acknowledgments: This work was funded by the Medical Research Council UK (MR/M006468/1, MR/L019248/1, and MR/S003207/1). RJC is funded by EPSRC Fellowship EP/N025946/1

Abstract

Topographic cortical maps are essential for spatial localisation of sensory stimulation and generation of appropriate task-related motor responses. Somatosensation and nociception are finely mapped and aligned in the adult somatosensory (S1) cortex, but in infancy, when pain behaviour is disorganised and poorly directed, nociceptive maps may be less refined. We compared the topographic pattern of S1 activation following noxious (clinically required heel lance) and innocuous (touch) mechanical stimulation of the same skin region in newborn infants (n=32) using multi-optode functional near-infrared spectroscopy (fNIRS). Signal to noise ratio and overall activation area did not differ with stimulus modality. Within S1 cortex, touch and lance of the heel elicit localised, partially overlapping increases in oxygenated haemoglobin (HbO), but while touch activation was restricted to the heel area, lance activation extended into cortical hand regions. The data reveals a widespread cortical nociceptive map in infant S1, consistent with their poorly directed pain behaviour.

Introduction

Somatotopically organised cortical maps of activity evoked by innocuous or noxious mechanical stimulation allow us to localise our sense of touch or pain (Penfield and Boldrey, 1937; Harding-Forrester and Feldman, 2018), and may also convey computational advantages in the relay of afferent information to higher brain areas (Thivierge and Marcus, 2007). In adults, overlapping regions are involved in the cortical processing of noxious and innocuous mechanical stimulation (Kenshalo et al., 2000; Lui et al., 2008) and detailed fMRI analysis reveals a fine-grained somatotopy for nociceptive inputs in primary somatosensory cortex (SI) that are aligned with activation maps following tactile stimuli, suggesting comparable cortical representations for mechanoreceptive and nociceptive signals (Mancini et al., 2012).

A whole-body topographical map of innocuous mechanical stimulation develops in the sensorimotor cortices over the early postnatal period in rats, which represent the human final gestational trimester (Seelke et al., 2012). Distinct representations of the hands and feet can be observed from 31 weeks using fMRI (Dall'Orso et al., 2018), becoming increasingly localised by term age (Allievi et al., 2016). While haemodynamic responses to a clinically-required heel lance have been recorded from 28 weeks using functional near-infrared spectroscopy (Slater et al., 2006) and can be distinguished from innocuous mechanical evoked brain activity in EEG recordings from 34-35 weeks (Fabrizi et al., 2011), the source of this activity and topographic representation of these two modalities have not been mapped, or their alignment established, in the infant cortex.

Infant pain behaviour is exaggerated and disorganised in newborn rodents and human infants (Fitzgerald, 2005, 2015; Cornelissen et al., 2013). Poor spatial tuning of nociceptive reflexes and receptive fields is a feature of the developing somatosensory system, followed by the emergence of adult organisation through activity-dependent refinement of synaptic connections (Beggs et al., 2002; Schouenborg, 2008; Koch and Fitzgerald, 2013). We hypothesised that this developmental process is reflected in ascending nociceptive signals to SI, leading to widespread cortical activation and poor spatial localisation of noxious events in early life.

To test this hypothesis, we used multioptode functional near-infrared spectroscopy (fNIRS) to map nociceptive and innocuous mechanoreceptive activity across the infant sensorimotor cortex. fNIRS is a non-invasive measure of cerebral haemodynamic changes which can be performed at the bedside, using skin-to skin holding in a naturalistic hospital setting during clinically required procedures. Using the temporal and spatial profiles of haemodynamic responses to a noxious skin lance and an innocuous touch of the hand and the heel, we show that haemodynamic activity elicited by noxious and innocuous mechanical stimulus have partially overlapping topographies in the human infant S1 cortex but that the two maps are not aligned. Noxious stimulation of the heel in the newborn evokes a more widespread cortical activation than innocuous stimulation, that extends into inferior regions of S1, normally associated with representation of the hand.

Results

Hand and heel touch evoked activity is somatotopically organised in the newborn infant S1 cortex

We first established the cortical topography of touch activation in newborn infants by mapping the extent of activation in the contralateral somatosensory (S1) cortex following innocuous mechanical stimulation (touch) of the hand and of the heel. **Figure 1a** and **1b** show a significant and localised increase in average [HbO] in contralateral optode channels following touch of each body area (n=11, hand touch; n=16 heel touch). Touch stimulation of the hand elicited significant increases in five channels, with a maximum change (0.31 μM at 16.9 s post-stimulus) at the channel corresponding to the FCC3 position of the 10:5 placement system (Figure 4), while touch of the foot elicited significant increases in six channels, with a maximum change (0.30 μM at 15.8 s) at the channel corresponding to the CPP1 10:5 position. The somatotopically localised increases in [HbO] were accompanied by

a widespread decrease in [Hb] over the whole peri-rolandic area (hand: significant decreases in eight channels [peak change: -0.21 μM at 17.7 s]; foot: significant decreases in nine channels, including control channel [peak change: -0.20 μM at 11.2 s]). An inverse response (significant decrease in [HbO], significant increase in [Hb], or both) was mostly restricted to channels surrounding the hand and foot areas of the S1, respectively. Individual channel data is shown in **Figure 1 – Source Data 1**.

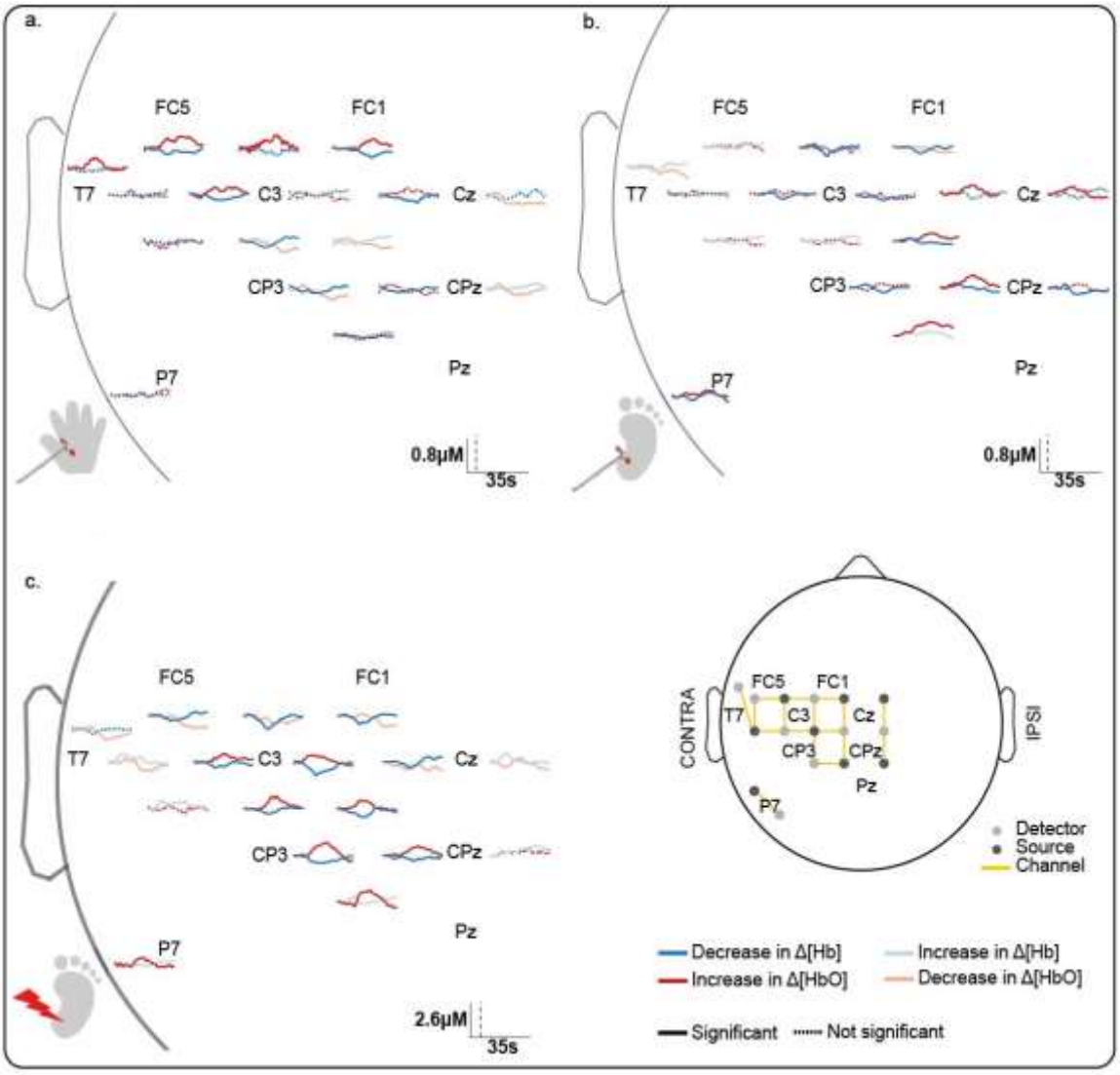

Figure 1. Channel-wise haemodynamic response following innocuous and noxious mechanical stimulation of hand and heel. *Average ⊿[HbO] (red) and ⊿[Hb] (blue) during (a) hand touch (n=11), (b) heel touch (n=16) and (c) heel lance (n=11). Channels with significant increases in [HbO] and decreases in [Hb] (i.e. canonical response) during the activation period are shown with sold dark lines, inverse responses are shown with solid pale lines, and non-significant changes are shown with dotted lines. Black vertical line represents stimulus onset. Note the difference in the scale bar between touch and lance. For channels where a significant canonical and inverse response was found at different latencies, the canonical response only is depicted. (Details of individual channel responses are in **Figure 1 – Source Data 1**)*

Image reconstruction of the channel data (Figure 2a and 2b) shows that the topography of touch activation in the newborn infant S1 is consistent with the known adult S1 topography: the area representing the foot lies in the superomedial postcentral gyrus, while the area for the hand is more inferior (Penfield and Boldrey, 1937; Harding-Forrester and Feldman, 2018; Willoughby et al., 2020).

Noxious lance of the heel elicits widespread activation extending into inferior SI

We next mapped activation in the contralateral S1 following a noxious, clinically required, lance stimulus to the heel in newborn infants. The average channel response (**Figure 1c**) and the image reconstruction (**Figure 2c**) show the significant and widespread increase in [HbO] following lancing the heel, which extends beyond the somatotopic area for heel touch to encompass inferior areas of SI, which were associated with touch of the hand.
Heel lance elicited significant increases in [HbO] in eight channels (including the control channel), with a maximum increase (0.96 μM at 14.5 s) at the channel corresponding to the CP2h 10:5 position. Four of the channels with a significant increase in [HbO] following the lance, also had a significant increase in [HbO] following touch of the foot. Notably one channel also displayed a significant increase following touch of the hand. The accompanying decrease in [Hb] was widespread (significant decreases in 11 channels; peak change 1.03 μM at 9.1 s), and an inverse response was found in all channels surrounding those with a canonical response (**Figure 1c and 2c**).

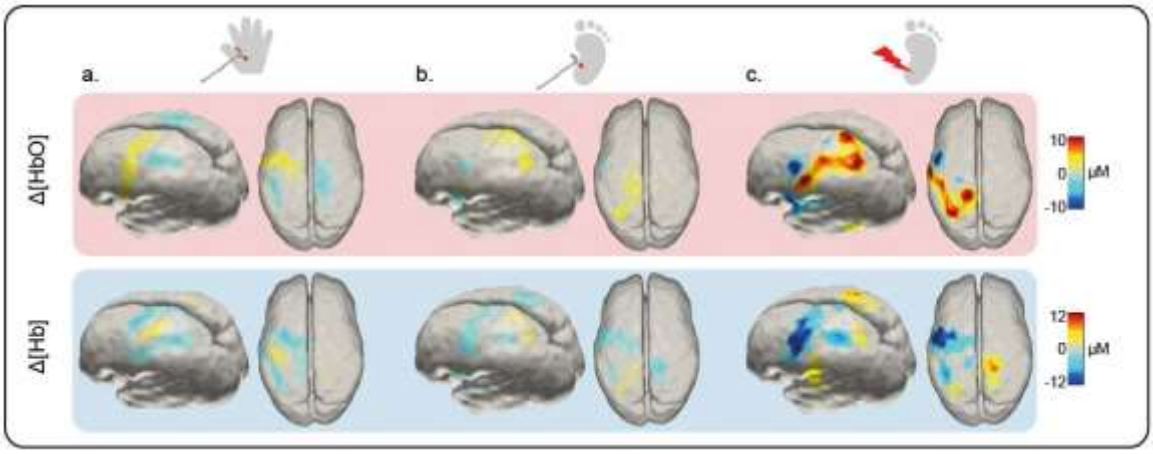

Figure 2. Image reconstruction at peak latency of the Δ[HbO] and Δ[Hb] response to an innocuous (touch) and noxious (lance) mechanical stimulation of hand and heel.
Significant changes (compared to baseline) in Δ[HbO] (top row) and Δ[Hb] (bottom row) following (a) hand touch (n=11), (b) heel touch (n=16) and (c) heel lance (n=11).

Newborn infant nociceptive maps are not somatotopically aligned with touch maps

To test whether the widespread activity evoked by heel lance within S1 represents a true difference in the somatotopic mapping of touch and nociception, we compared the signal to noise, the individual channel activation and the overall spatial dimensions of haemodynamic activity evoked by the two stimulus modalities applied to the heel.
Heel lance elicited a significantly larger increase in [HbO] and decrease in [Hb] compared to heel touch (maximum Δ[HbO]: 15.23 vs 4.13 μM, p=.007; maximum Δ[Hb]: -22.87 vs -4.34 μM, p<.001; **Figure 3b, Figure 3 – figure supplement 1**). However, the signal to noise of the lance heel activation was not higher than that of heel touch evoked activity (see Methods). Furthermore, the difference in amplitude between lance and touch was not accompanied by a difference in overall area of cortical activation evoked by the two stimuli (**Figure 3b and Figure 3 – Source Data 1**). Neither the location nor latency of peak activation differed between the two stimulus modalities (Δ [HbO]: distance between peaks = 1.65 mm, p=.776; difference in peak latency = 1.7 s [14.1 vs 15.8 s], p=.356; Δ [Hb]: distance between peaks = 0 mm, p=.957; difference in peak latency = 1.7 s [9.6 vs 11.3 s], p=.292). Only the spread of the peak Δ [HbO] was significantly larger following noxious heel lance (Δ [HbO] FWHM area: 66.63 vs 52.96 mm2, p=.015; Δ [Hb] FWHM area: 87.86 vs 83.10 mm2, p=.204). (Figure 3 – figure supplement 1). The key difference between the two patterns of

activation is that the foot touch response is limited to the areas of the S1/M1 associated with the foot, whereas the lance response extends towards other more ventral regions of S1.

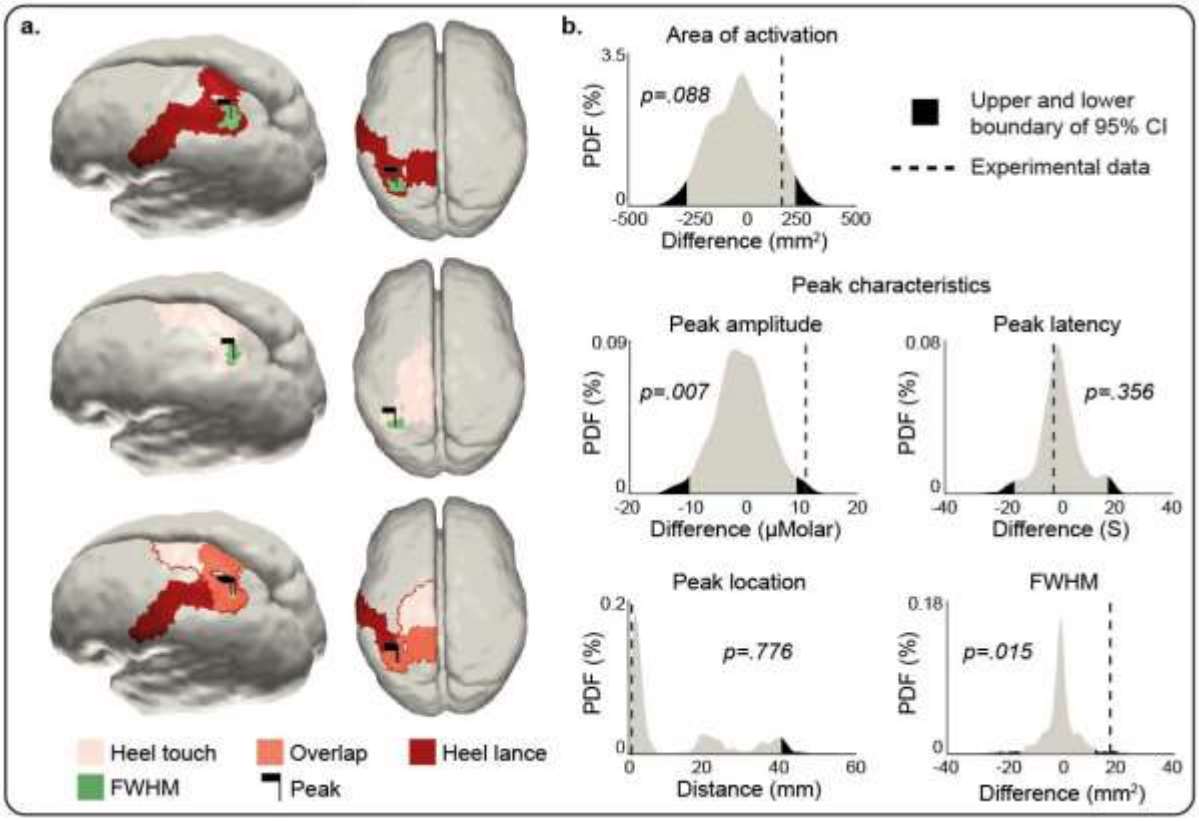

Figure 3. Comparison of the peak and area of activation of the Δ[HbO] response to an innocuous (touch) and noxious (lance) mechanical stimulation of the heel. (*a) Area of significant Δ[HbO] changes following heel lance (red), heel touch (pink) and both (orange). Black flags demark the location of peak changes and green areas the extent of their full-width half-maximum (FWHM). (b) Statistical position of experimental differences between heel touch and lance in peak amplitude, FWHM, latency and location, and area of significant Δ[HbO] changes in respect to non-parametric null distributions obtained with bootstrapping and phase scrambling. The equivalent plots for Δ[Hb] are shown in **Figure 3 - figure supplement 1** and **Figure 3 - source data 1**.*

Discussion

A widespread nociceptive topographic map in infant S1 that overlaps but is not aligned to the innocuous mechanoreceptive map

Somatosensory maps of cortical activity evoked by a cutaneous tactile or noxious stimulus provide a framework for localising the sense of touch or pain (Treede et al., 1999; Thivierge and Marcus, 2007). The adult primate S1 has a defined somatotopic organization of tactile and nociceptive cortical receptive fields (Andersson et al., 1997; Kenshalo et al., 2000) including spatially precise cortical maps of Aδ and Aβ afferent fibre input (Chen et al., 2011). Human fMRI studies show that adult somatotopic maps of noxious and non-noxious mechanical stimulation substantially overlap (Lui et al., 2008) and detailed analysis reveals a fine-grained somatotopy for nociceptive inputs in primary somatosensory cortex (S1) that are highly aligned with maps of innocuous tactile stimuli, suggesting comparable cortical representations for mechanoreceptive and nociceptive signals (Mancini et al., 2012). Here we have shown that this comparable representation is not present in the newborn infant S1 cortex.

Noxious mechanical stimulation evokes a larger peak increase in Δ[HbO] and decrease in Δ[Hb] compared to innocuous stimulation of the same body area at comparable location and latency as reported elsewhere (Bartocci et al., 2006; Slater et al., 2006; Verriotis et al., 2016b). The fact that the noxious activation is greater than the touch evoked activity (clearly seen because fNIRS provides scaled maps of the physiologically meaningful parameter, haemoglobin concentrations, unlike BOLD-fMRI) is presumably due to greater depolarisation and spike activity within the activated areas. However, it does not explain the differing topography reported here. The signal to noise ratio is not larger following noxious stimulation as we averaged data from repeated touches to compare with a single lance stimulus. Furthermore, the overall area of brain activity does not differ significantly between touch and lance of the heel, it is only that the areas of activation of the responses are not aligned. Within S1 itself, the infant has a distinct somatotopic map for touch, similar to that described in adults, with the area representing the foot lying in the superomedial postcentral gyrus, and the area for the hand located more inferiorly (Penfield and Boldrey, 1937; Blake et al., 2002; Akselrod et al., 2017), consistent with previous reports in newborn infants (Dall'Orso et al., 2018). Noxious heel lance, on the other hand, evokes a widespread activity within S1 , peaking in the same area of the superomedial postcentral gyrus as touch activity, but extending to the hand representation area. The multi-optode fNIRS array was placed over the contralateral perirolandic cortex and so the full extent of the nociceptive map is not known, but the data shows that the S1 somatotopic nociceptive map is not as precise as the touch map in the newborn.

Measuring the cortical haemodynamic response to innocuous and noxious mechanical stimulation in neonates

fNIRS is ideally suited to a study of this kind as recording and sensory stimulation, including clinically required heel lance, can be performed at the infant cotside (Bartocci et al., 2006; Slater et al., 2010; Kashou et al., 2016; Verriotis et al., 2016b). Other methods of measuring this either do not provide sufficient spatial information and source localisation, such as EEG recording of nociceptive-related ERPs (Fabrizi et al., 2011; Jones et al., 2018) or are limited by the use experimental 'pinprick' stimulators, that for ethical reasons are not actually painful, such as in fMRI studies (Goksan et al., 2015).

The change in the Δ[HbO] and Δ[Hb] following sensory stimulation is a measure of neural activity: simultaneous vertex EEG and fNIRS recordings over S1 show that haemodynamic and neural responses are related in magnitude (Verriotis et al., 2016b). Following all stimuli, and consistent with the mature canonical response, channels showing a significant increase in Δ[HbO] also had a smaller decrease in Δ[Hb]. Regional overperfusion following neuronal activation, beyond that required by metabolic demands, means that less Hb is removed from the region compared to the oversupply of HbO. However, the decrease in Δ[Hb] was more widespread (but smaller in magnitude) compared to the localised increase in Δ[HbO]. This type of response, not previously reported in infants (de Roever et al., 2018), suggests that more blood is leaving the region (removing Hb) compared to the incoming supply (no significant change in [HbO] in peripheral channels) due to immature regulation of cerebral blood flow (CBF). There are multiple mechanisms by which blood vessels dilate and CBF increases following neural activation, including arterial CO_2 and O_2 concentrations, which relax/contract the smooth muscle cells of cerebral arteries and arterioles (Kety and Schmidt, 1948), and astrocyte and pericyte activity which contribute to vessel diameter and the propagation of vasodilation along the vascular tree (Takano et al., 2006; Cai et al., 2018), many of which are still developing in the newborn (Pryds and Greisen, 1989; Binmöller and Müller, 1992; Fujimoto, 1995) leading to rapid changes in CBF over the first postnatal days as cerebral circulation adapts (Meek et al., 1998).

These infants in this study were held skin to skin, swaddled in their mother's arms in a naturalistic setting, which is a major advantage of nIRS recording over fMRI for human developmental studies of brain function. Video recording and investigator scoring confirmed that while some infant movement and maternal touching did take place and that some

babies did move following the lance, these movements were varied in both body part and latency such that any associated cortical response would be removed during the averaging process. Furthermore, the chance of any larger movement from a few babies driving the widespread S1 response following the lance, is removed by the between group randomisation used to generate the null distribution of parameter differences. Finally, 33--50% of babies did grimace for up to 7 seconds following the lance, but if these facial movements mediated the response following the lance, this would have prolonged the peak or duration of the change in HbO, while in fact the latency and time course of the response to both stimuli was the same (see Figure 1).

Differential development of somatosensory and nociceptive topographic maps

A whole-body topographical map of innocuous mechanical stimulation develops in the sensorimotor cortices over the early postnatal period in rats (Seelke et al., 2012), which represents the human final gestational trimester. In humans, distinct representations of the hands and feet can be observed from 31 weeks gestation, using fMRI (Dall'Orso et al., 2018), and from 28 weeks using neural activity recorded from the scalp (Donadio et al., 2018; Whitehead et al., 2018, 2019). The response to innocuous mechanical stimulation was more localised in S1 than the wider and less refined topographical map of noxious mechanical stimulation, suggesting a slower maturation of the S1 circuitry involved in nociceptive processing compared to touch processing in the infant brain.

In rodents, at every level of the developing somatosensory central nervous system, tactile processing matures before nociceptive processing (Fitzgerald, 2005; Koch and Fitzgerald, 2013; Chang et al., 2016, 2020; Verriotis et al., 2016a) consistent with a delayed refinement of a cortical nociceptive map. Widespread nociceptive cortical maps are consistent with infant pain behaviour, characterised by exaggerated and disorganised nociceptive reflexes in both rodent pups and human neonates (Fitzgerald, 2005, 2015), and which can fail to remove a body part from the source of pain (Waldenström et al., 2003). Nociceptive reflexes following noxious heel lance are larger in magnitude and significantly more prolonged in human infants compared to adults (Cornelissen et al., 2013) and have widespread cutaneous receptive fields that encompass the whole lower limb (Andrews and Fitzgerald, 1994). This lack of organisation could be reflected in the ascending spinothalamic and thalamocortical projections, delaying the maturation of S1 cortical nociceptive maps in the newborn. Topographic maps are established and aligned via multiple mechanisms, including molecular cues, spontaneous or sensory-dependent remodelling, and refinement. Initially, somatosensory maps are diffuse and overlapping, but in the rodent somatosensory cortex, excitatory thalamocortical afferents undergo activity-dependent refinement to sharpen these maps (Iwasato et al., 1997). Equally important is the maturation of inhibitory interneuron sensory maps which, in contrast, expand over development in an experience dependent manner (Quast et al., 2017). Slow developmental broadening of an inhibitory nociceptive network may explain the widespread nociceptive map in S1 and also the greater amplitude of EEG noxious responses in infants compared to adults (Fabrizi et al., 2016).

Pain and the developing S1 cortex

This study highlights the importance of understanding the development of touch and pain processing in the human infant brain. The widespread S1 nociceptive topography discovered here implies that the infant S1 cortex would be unable to accurately localise noxious events and may lack the computational ability to reliably send noxious information to higher brain centres (Thivierge and Marcus, 2007; Harding-Forrester and Feldman, 2018). Heel lance is one of many skin-breaking procedures commonly performed in neonatal hospital care (Laudiano-Dray et al., 2020) and this study reveals the extent of cortical activation that follows just one such noxious procedure in the newborn. This contrasts with innocuous mechanical stimulation, such as touch, which activates a spatially restricted and somatotopically defined cortical area. Increasing evidence that repeated noxious experiences have adverse effects upon the developing brain (Ranger and Grunau, 2014;

Duerden et al., 2018), underlines the importance of these results and the need for a better understanding of the mechanisms underlying the maturation of cortical nociceptive topographic maps.

Materials and Methods

Participants

Thirty-two infants (35-42 gestational weeks at birth, 0-7 days old, 12 female; **Table 1**) were recruited from the postnatal, special care, and high dependency wards within the neonatal unit at University College London Hospital. Infants received either 1) innocuous mechanical stimulation (touch) of the heel, 2) innocuous mechanical stimulation of the hand, or 3) a noxious mechanical stimulation (clinically required lance) of the heel. Six infants received touch stimulation of both the heel and hand. Similar high impact works using single trial noxious stimulation or multiple mechanical stimulations have yielded significant results with group sample sizes of 5-15 (Bartocci et al.,2006) and 10-15 (Arichi et al., 2012), respectively. Ethical approval for this study was given by the NHS Health Research Authority (London – Surrey Borders) and the study conformed to the standards set by the Declaration of Helsinki. Informed written parental consent was obtained before each study.

Table 1. Infant demographics. Demographic information about the subjects that received tactile and noxious stimuli of heel and hand.

	Heel lance	Heel touch	Hand touch	p
N	11	16	11	
GA (weeks^{+days})	39^{+2} (35^{+2} – 41^{+5})	39^{+4} (35 – 42^{+3})	39^{+2} (37^{+5} – 41^{+3})	.287
PNA (days)	4 (0 - 7)	3 (0 - 6)	3 (0 - 4)	.115
Females	4 (36%)	6 (38%)	5 (45%)	.889
Birth weight (g)	3134 (2220 - 4072)	3250 (2360 - 4080)	3300 (2450 - 3754)	.774
Caesarean deliveries	2 (18%)	8 (50%)	3 (27%)	.196
Head circumference (cm)	34 (32 – 35.5)	34.25 (31 - 37)	34 (32.5 - 36)	.900

Values represent median and range or proportion. GA = gestational age (weeks from the first day of the mothers last menstrual cycle to birth); PNA = postnatal age (days since birth). No significant difference was found in any demographic parameter across the three groups (one-way ANOVA results in the last column).

Experimental design

Brain activity (fNIRS) was recorded following a clinically-required heel lance procedure or innocuous mechanical stimulation of the limbs at the bedside in the neonatal unit.

Functional Near-Infrared Spectroscopy recording

Infants wore a 21-channel array consisting of 8 sources and 8 detectors with inter-optode distances of 2.5-4 cm. The array was secured over the pericentral area of the scalp on the side contralateral to the stimulation with a custom designed textile cap (EasyCap). The infants' head circumference, ear to ear lateral semi circumference, and nasion to inion distance were measured and the cap was placed on the head by aligning specific 10/5 locations (Cz, T7). This optode arrangement provided sensitivity coverage for the whole somatomotor cortex contralateral to the stimulation site and of the medial part on the ipsilateral side (**Figure 4c**). One source-detector pair was placed at a more ventral posterior location of the scalp (P7 of the international 10/5 positioning system) (**Figure 4a**). This channel was sensitive to the posterior temporal lobe and worked as a control channel (**Figure 4b and 4c**). A continuous wave recording system was used with 2 wavelengths of

source light at 780nm and 850nm and a sampling rate of 10Hz to measure changes in oxy- and deoxy-haemoglobin concentration (Gowerlabs NTS fNIRS system).

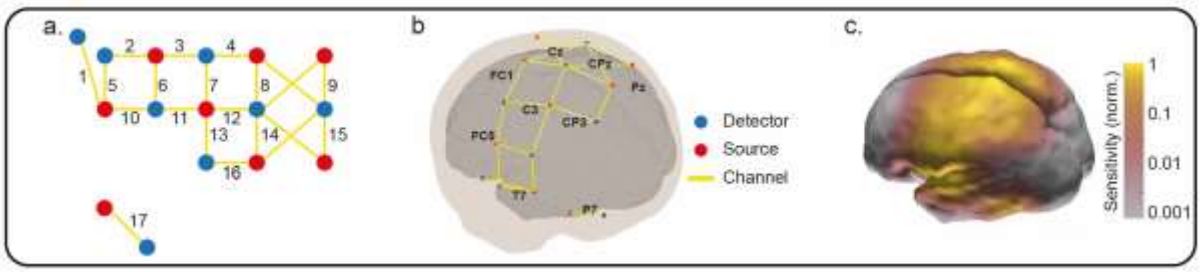

Figure 4. Optode locations and sensitivity map *(a) Channel reference numbers for Figure 1 – source data 1. (b) Locations of the fNIRS sources, detectors and resulting measurement channels registered to a 39-week anatomical atlas. (c) Normalized fNIRS sensitivity illustrating the spatial coverage provided by the channel arrangement in panel (b). This sensitivity map was calculated using the photon measurement density functions derived from the TOAST++ light transport modelling package.*

Noxious mechanical stimulation

The noxious stimulus was a clinically required heel lance for blood sampling. Blade release was time-locked to the NIRS recording using an accelerometer attached to the lancet (Worley et al., 2012). The lancet was placed against the heel for at least 30s prior to the release of the blade. This was to obtain a baseline period free from other stimulation. The heel was then squeezed 30s after the release of the blade, again to ensure a post-stimulus period free from other stimuli. All lances were performed by the same trained nurse (MPL-D) using a disposable lancet, and standard hospital practice was followed at all times.

Innocuous mechanical stimulation

Innocuous mechanical stimulation was delivered by light touch on the lateral edge of the infants' palms and/or heels using a hand-held tendon hammer (ADInstruments). A piezo-electric sensor mounted on the hammer head provided a synchronising signal to the NIRS recording. A train of up to 15 touches (average = 11.5) was delivered to each limb with a variable inter-stimulus interval of 35 – 60 seconds. If the infant moved in the 30s pre- or post-stimulus the trial was removed (heel: average of 1.4 touches were removed in 8/16 infants; hand: average of 1.5 touches removed in 11/11 infants). This resulted in an average of 10.1 heel touches (range = 7 – 13) and 9.3 hand touches (range = 5 – 11) per infant.

Recording infant movements

All infants were prone against their mother's chest. The mother, who was inclined on a chair or bed, was instructed to avoid moving or stimulating the infant during the 1 minute before and after the release of the lance. Movements were minimized as infants were

swaddled (wrapped securely in clothes/blankets) against the mother's chest and the research nurse was holding the exposed foot throughout the period before and after the stimulus.

Table 2. **Infant movements.** The number of infants who displayed movements or received tactile stimulation from their mother each second in the 30s following lance.

	Number of infant and maternal movements						
Post-lance (s)	**Hand**	**Head**	**Face**	**Foot**	**Arm**	**Mother touching face**	**Mother touching head**
1	1	1	4	0	2	1	1
2	1	1	6	1	2	1	1
3	1	0	6	1	2	1	1
4	1	0	6	0	2	1	1
5	1	1	6	0	2	1	1
6	1	1	6	0	2	1	0
7	0	1	4	0	1	1	0
8	0	1	3	0	1	1	0
9	0	1	2	0	1	1	0
10	0	0	1	0	1	1	0
11	0	0	1	0	1	1	0
12	0	0	1	0	1	1	0
13	0	0	1	0	1	1	0
14	0	0	1	0	1	1	0
15	0	0	1	0	0	1	0
16	0	0	1	0	0	1	0
17	0	0	0	0	0	1	0
18	0	0	0	0	0	1	0
19	0	0	0	0	0	1	0
20	0	0	0	0	0	1	0
21	0	0	0	0	0	1	0
22	0	0	0	0	0	1	0
23	0	0	0	0	0	1	0
24	0	0	0	0	0	1	0
25	0	0	0	0	0	1	0
26	0	0	0	0	0	1	0
27	0	0	0	0	0	1	0
28	0	0	0	0	0	1	0
29	0	0	0	0	0	1	0
30	0	0	0	0	0	1	0

Each movement or stimulation was scored as present (1) or not present (0) per infant, and the value in each cell represents the total number of infants (out of 11) for whom each movement or stimulation was observed.

Infant movements, or changing tactile stimulation were recorded on video, which was synchronised with the NIRS recording using an LED light within the frame that was activated by the release of the lance (Worley et al., 2012). In case movements were obscured, a second researcher also recorded movements at the time of the study using a stopwatch. Movements or tactile stimulation were separated into body parts and coded per second as either 0 (not present) or 1 (present) for the 30 s post-stimulus. The total number of babies

displaying each type of movement at each second post-lance can be seen in Table 2. Following the lance, 2 babies did not move, 6 babies made small movements (including: small or brief grimace, head nod, twitch, small hand movement), 4 babies made larger movements (including arms, large or prolonged grimace, nod of head), and 2 babies received tactile stimulation from the mother (including: positioning the head, stroking the face).

Data pre-processing

All data were pre-processed in Homer2 (Huppert and Boas, 2005). Light intensity data were inspected for poor signal quality (signal intensity < 0.01, SNR < 2) resulting in 9 individual channels across lance trials (4%) being removed from further analysis, 12 across the heel touch trials (4%), and 6 across the hand touch trials (3%). Due to poor signal quality in the majority of trials, the 4 channels crossing over the midline were removed from all trials (**Figure 4a and 4b)**. Data were then converted into optical density, motion artefacts were detected (change in amplitude > 0.7 and/or change in standard deviation > 15 over a 1s time period) and then corrected using Wavelet filtering (Molavi and Dumont, 2012). Instrumental drift and cardiac artefact were removed with a 0.01-0.5 Hz bandpass filter. Optical density changes recorded from all channels (likely related to stimulus dependent systemic physiological changes) were removed using Principal Component Analysis ((Kozberg and Hillman, 2016; Tachtsidis and Scholkmann, 2016); 1 component removed). Finally, data were converted into changes in oxy- and deoxy-haemoglobin concentration (Δ[HbO] and Δ[Hb]) using the modified Beer–Lambert law (Delpy et al., 1988) with a differential path-length factor of 4.39 (Wyatt et al., 1990). The continuous signal was then epoched from -5 to 30 s around the noxious and somatosensory stimuli. Somatosensory stimuli were averaged for each subject.

Signal to Noise

The signal to noise ratio (SNR) for lance and for touch were calculated. Despite the peak signal for lance being higher, the SNR is lower, because more touch trials were averaged in this study. The ratio of lance to touch SNR ($(peak_{lance}/peak_{touch})*(sqrt(n_{lance})/sqrt(n_{touch})$ = (0.96/0.30) * (sqrt(11)/sqrt(157)) = 0.85.

Channel-wise data analysis

Pre-processed data were then averaged across subjects for each condition and analysed using custom MATLAB scripts (Mathworks; version 16b). For each channel, significant changes in Δ[HbO] and Δ[Hb] were identified with a two-tailed t-test (α = 0.01) comparing each time point post-stimulus against the baseline. This baseline distribution was calculated as the mean of the individual baselines (-5 – 0s before stimulus) according to:

$$\frac{1}{S}\sum_{i=1}^{S} x_i \sim N\left(\frac{1}{S}\sum_{i=1}^{S}\mu_i, \frac{1}{S^2}\sum_{i=1}^{S}\sigma_i^2\right).$$

Where S is the number of subjects and $x_i \sim N(\mu_i, \sigma_i^2)$ is the baseline for subject i.

Bonferroni correction was used for multiple comparisons (17 channels x 300 samples = 5100 comparisons). Only changes (increases or decreases) which were continuously significant for at least 1 second (10% of the length of the post-lance period) were retained (Guthrie and Buchwald, 1991).

Data analysis in image space

Image reconstruction

The channel-wise data was used to create functional images using a cortically constrained linear reconstruction approach. The fNIRS array was registered to a 39-week gestational age anatomical mesh model with 784391 nodes (Brigadoi et al., 2014) using tools from the AtlasViewer package (Aasted et al., 2015). Images were reconstructed using the DOT-HUB toolbox (www.github.com/DOT-HUB) and the TOAST++ light transport modelling package (Schweiger and Arridge, 2014) (www.github.com/toastpp), with zeroth-order Tikhonov regularization with a regularization hyperparameter of 0.1.

Assessment of changes in Δ[HbO] and Δ[Hb]

We first assessed the significance of the changes in Δ[HbO] and Δ[Hb] elicited by heel and hand touch and heel lance compared to baseline in image space. To do that, we reconstructed image time-series (i.e. one image reconstructed at each time-point) for each subject/stimulus. For each node, significant peak reconstructed changes in Δ[HbO] and Δ[Hb] were identified with a two-tailed t-test ($\alpha = 0.01$) comparing the peak time point within a 5-second window around the peak latency derived from the channel-wise analysis against the baseline. As in channel-wise analysis this baseline distribution was calculated as the mean of the individual baselines (-5 – 0s pre-stimulus). Bonferroni correction was used for multiple comparisons (784391 nodes = 784391 comparisons). To display these results we: (1) reconstructed an image using the average channel-wise data within the 5-second window around the peak latency (averaged in time) for hand touch, heel touch and lance and (2) masked this image according to the result of the statistical test above.

Comparison of changes in Δ[HbO] and Δ[Hb] between heel lance and touch

Next, we wanted to compare the peak changes in Δ[HbO] and Δ[Hb] between the heel lance and touch conditions in image space. To do this, we calculated the difference in overall area of activation, and magnitude, latency, location, and spread of the peak change in Δ[HbO] and Δ[Hb], and compared these against a non-parametric null distribution.

Area of activation was defined as the cortical surface area with significant Δ[HbO] (or Δ[Hb]) changes. Difference in peak location was the Euclidean distance between the peaks. Peak spread was defined as the cortical surface area around the peak where changes in Δ[HbO] (or Δ[Hb]) were at least half of the peak change (full-width half-maximum, FWHM). Cortical surface areas (area of activation and peak spread) were defined by starting at the node with the peak change and continually expanding to include neighbouring nodes that were (1) connected by at least 2/3 face edges, and (2) had a significant change from baseline.

The non-parametric null distribution was derived by calculating these differences between randomly selected sets of surrogate image time-series (bootstrapping on surrogate data). We here describe how we obtained surrogate image time-series and then how we conducted bootstrapping.

Each individual recording (i.e image time-series) can be considered as the linear sum of a signal of interest (i.e. the response to the stimulus) and a stationary random noise component. The assumption is that the signal is the same in each recording while the noise changes. Therefore, if we were to conduct another recording on another subject the new data would be the linear sum of the *same* signal that we find in the original data but *different* random noise. Creating surrogate data consists in generating new random noise to add to the signal estimated from our data. To do this we: (1) estimate the signal by averaging across individual recordings (i.e. subjects) in response to the same stimulus modality; (2) isolate the noise in our data by subtracting this estimate from each recording; (3) *phase-randomise* each noise time-series. Phase-randomization is applied independently to each node time-series in the frequency-domain. This means that the phase component of the complex-valued signal is rotated at each frequency by an independent random variable chosen from the uniformly distributed range of 0 and 2π (Theiler et al., 1992). At the end of this process we have a new set of surrogate noise time-series.

To generate the full non-parametric null distribution against which to compare our data, we used bootstrapping. To estimate each sample of the null distribution, we calculated the differences in area of activation and peak amplitude, latency, position and FWHM between two random sets of surrogate data without any systematic difference. To create the random sets, we: (1) pooled together all the newly obtained surrogate noise time-series; (2) added the grand average (across lance and touch) signal (as we do not want systematic differences between sets to estimate a null distribution); (3) randomly split (with repetition) these surrogate data into two sets. We repeated this 1000 times in order to obtain the full non-parametric null distribution (bootstrapping). An experimental difference outside the 95% confidence interval was considered significant ($p < 0.05$).

Data sharing

All raw data files are open access and are available to download from Figshare (https://doi.org/10.6084/m9.figshare.13252388.v2).

References

Aasted CM, Yücel MA, Cooper RJ, Dubb J, Tsuzuki D, Becerra L, Petkov MP, Borsook D, Dan I, Boas DA (2015) Anatomical guidance for functional near-infrared spectroscopy: AtlasViewer tutorial. Neurophotonics 2:020801.

Akselrod M, Martuzzi R, Serino A, van der Zwaag W, Gassert R, Blanke O (2017) Anatomical and functional properties of the foot and leg representation in areas 3b, 1 and 2 of primary somatosensory cortex in humans: A 7T fMRI study. NeuroImage 159:473–487.

Allievi AG, Arichi T, Tusor N, Kimpton J, Arulkumaran S, Counsell SJ, Edwards AD, Burdet E (2016) Maturation of Sensori-Motor Functional Responses in the Preterm Brain. Cereb Cortex 26:402–413.

Andersson JL, Lilja A, Hartvig P, Långström B, Gordh T, Handwerker H, Torebjörk E (1997) Somatotopic organization along the central sulcus, for pain localization in humans, as revealed by positron emission tomography. Exp Brain Res 117:192–199.

Andrews K, Fitzgerald M (1994) The cutaneous withdrawal reflex in human neonates: sensitization, receptive fields, and the effects of contralateral stimulation. Pain 56:95–101.

Arichi T, Fagiolo G, Varela M, Melendez-Calderon A, Allievi A, Merchant N, Tusor N, Counsell SJ, Burdet E, Beckmann CF, Edwards AD (2012) Development of BOLD signal hemodynamic responses in the human brain. NeuroImage 63:663–673.

Bartocci M, Bergqvist LL, Lagercrantz H, Anand KJS (2006) Pain activates cortical areas in the preterm newborn brain: Pain 122:109–117.

Beggs S, Torsney C, Drew LJ, Fitzgerald M (2002) The postnatal reorganization of primary afferent input and dorsal horn cell receptive fields in the rat spinal cord is an activity-dependent process. Eur J Neurosci 16:1249–1258.

Bembich S, Brovedani P, Cont G, Travan L, Grassi V, Demarini S (2015) Pain activates a defined area of the somatosensory and motor cortex in newborn infants. Acta Paediatr Oslo Nor 1992 104:e530-533.

Bembich S, Marrazzo F, Barini A, Ravalico P, Cont G, Demarini S (2016) The cortical response to a noxious procedure changes over time in preterm infants. Pain 157:1979–1987.

Binmöller F-J, Müller CM (1992) Postnatal development of dye-coupling among astrocytes in rat visual cortex. Glia 6:127–137.

Blake DT, Byl NN, Merzenich MM (2002) Representation of the hand in the cerebral cortex. Behav Brain Res 135:179–184.

Brigadoi S, Aljabar P, Kuklisova-Murgasova M, Arridge SR, Cooper RJ (2014) A 4D neonatal head model for diffuse optical imaging of pre-term to term infants. NeuroImage 100:385–394.

Cai C, Fordsmann JC, Jensen SH, Gesslein B, Lønstrup M, Hald BO, Zambach SA, Brodin B, Lauritzen MJ (2018) Stimulation-induced increases in cerebral blood flow and local capillary vasoconstriction depend on conducted vascular responses. Proc Natl Acad Sci 115:E5796–E5804.

Chang P, Fabrizi L, Fitzgerald M (2020) Distinct Age-Dependent C Fiber-Driven Oscillatory Activity in the Rat Somatosensory Cortex. eNeuro 7.

Chang P, Fabrizi L, Olhede S, Fitzgerald M (2016) The Development of Nociceptive Network Activity in the Somatosensory Cortex of Freely Moving Rat Pups. Cereb Cortex N Y N 1991 26:4513–4523.

Chen LM, Dillenburger BC, Wang F, Friedman RM, Avison MJ (2011) High-resolution functional magnetic resonance imaging mapping of noxious heat and tactile activations along the central sulcus in New World monkeys. Pain 152:522–532.

Cornelissen L, Fabrizi L, Patten D, Worley A, Meek J, Boyd S, Slater R, Fitzgerald M (2013) Postnatal Temporal, Spatial and Modality Tuning of Nociceptive Cutaneous Flexion Reflexes in Human Infants. PLoS ONE 8 Available at: https://www.ncbi.nlm.nih.gov/pmc/articles/PMC3790695/ [Accessed January 21, 2019].

Dall'Orso S, Steinweg J, Allievi AG, Edwards AD, Burdet E, Arichi T (2018) Somatotopic Mapping of the Developing Sensorimotor Cortex in the Preterm Human Brain. Cereb Cortex 28:2507–2515.

de Roever I, Bale G, Mitra S, Meek J, Robertson NJ, Tachtsidis I (2018) Investigation of the Pattern of the Hemodynamic Response as Measured by Functional Near-Infrared Spectroscopy (fNIRS) Studies in Newborns, Less Than a Month Old: A Systematic Review. Front Hum Neurosci 12 Available at: https://www.ncbi.nlm.nih.gov/pmc/articles/PMC6176492/ [Accessed March 2, 2020].

Delpy DT, Cope M, Zee P van der, Arridge S, Wray S, Wyatt J (1988) Estimation of optical pathlength through tissue from direct time of flight measurement. Phys Med Biol 33:1433–1442.

Donadio A, Whitehead K, Gonzalez F, Wilhelm E, Formica D, Meek J, Fabrizi L, Burdet E (2018) A novel sensor design for accurate measurement of facial somatosensation in pre-term infants. PLOS ONE 13:e0207145.

Duerden EG, Grunau RE, Guo T, Foong J, Pearson A, Au-Young S, Lavoie R, Chakravarty MM, Chau V, Synnes A, Miller SP (2018) Early Procedural Pain Is Associated with Regionally-Specific Alterations in Thalamic Development in Preterm Neonates. J Neurosci Off J Soc Neurosci 38:878–886.

Fabrizi L, Slater R, Worley A, Meek J, Boyd S, Olhede S, Fitzgerald M (2011) A shift in sensory processing that enables the developing human brain to discriminate touch from pain. Curr Biol 21:1552–1558.

Fabrizi L, Verriotis M, Williams G, Lee A, Meek J, Olhede S, Fitzgerald M (2016) Encoding of mechanical nociception differs in the adult and infant brain. Sci Rep 6:28642.

Fitzgerald M (2005) The development of nociceptive circuits. Nat Rev Neurosci 6:507–520.

Fitzgerald M (2015) What do we really know about newborn infant pain? Exp Physiol 100:1451–1457.

Fujimoto K (1995) Pericyte-endothelial gap junctions in developing rat cerebral capillaries: A fine structural study. Anat Rec 242:562–565.

Goksan S, Hartley C, Emery F, Cockrill N, Poorun R, Moultrie F, Rogers R, Campbell J, Sanders M, Adams E, Clare S, Jenkinson M, Tracey I, Slater R (2015) fMRI reveals neural activity overlap between adult and infant pain. eLife 4:e06356.

Guthrie D, Buchwald JS (1991) Significance Testing of Difference Potentials. Psychophysiology 28:240–244.

Harding-Forrester S, Feldman DE (2018) Somatosensory maps. Handb Clin Neurol 151:73–102.

Huppert T, Boas DA (2005) HomER: Hemodynamic evoked response NIRS data analysis GUI. Available from the Photon Migration Imaging Lab. Martinos Cent Biomed Imaging Available at: http://www. nmr. mgh. harvard. edu/PMI.

Iwasato T, Erzurumlu RS, Huerta PT, Chen DF, Sasaoka T, Ulupinar E, Tonegawa S (1997) NMDA Receptor-Dependent Refinement of Somatotopic Maps. Neuron 19:1201–1210.

Jones L, Laudiano-Dray MP, Whitehead K, Verriotis M, Meek J, Fitzgerald M, Fabrizi L (2018) EEG, behavioural and physiological recordings following a painful procedure in human neonates. Sci Data 5:180248.

Kashou NH, Dar IA, Hasenstab KA, Nahhas RW, Jadcherla SR (2016) Somatic stimulation causes frontoparietal cortical changes in neonates: a functional near-infrared spectroscopy study. Neurophotonics 4:011004.

Kenshalo DR, Iwata K, Sholas M, Thomas DA (2000) Response properties and organization of nociceptive neurons in area 1 of monkey primary somatosensory cortex. J Neurophysiol 84:719–729.

586 Kety SS, Schmidt CF (1948) The effects of altered arterial tensions of carbon dioxide and
587 oxygen on cerebral blood flow and cerebral oxygen consumption of normal young
588 men. J Clin Invest 27:484–492.
589 Koch SC, Fitzgerald M (2013) Activity-dependent development of tactile and nociceptive
590 spinal cord circuits. Ann N Y Acad Sci 1279:97–102.
591 Kozberg M, Hillman E (2016) Chapter 10 - Neurovascular coupling and energy metabolism
592 in the developing brain. In: Progress in Brain Research (Masamoto K, Hirase H,
593 Yamada K, eds), pp 213–242 New Horizons in Neurovascular Coupling: A Bridge
594 Between Brain Circulation and Neural Plasticity. Elsevier. Available at:
595 http://www.sciencedirect.com/science/article/pii/S0079612316000376 [Accessed
596 September 24, 2019].
597 Laudiano-Dray MP, Pillai Riddell R, Jones L, Iyer R, Whitehead K, Fitzgerald M, Fabrizi L,
598 Meek J (2020) Quantification of neonatal procedural pain severity: a platform for
599 estimating total pain burden in individual infants. Pain 161:1270–1277.
600 Lui F, Duzzi D, Corradini M, Serafini M, Baraldi P, Porro CA (2008) Touch or pain? Spatio-
601 temporal patterns of cortical fMRI activity following brief mechanical stimuli: Pain
602 138:362–374.
603 Mancini F, Haggard P, Iannetti GD, Longo MR, Sereno MI (2012) Fine-grained nociceptive
604 maps in primary somatosensory cortex. J Neurosci Off J Soc Neurosci 32:17155–
605 17162.
606 Meek JH, Tyszczuk L, Elwell CE, Wyatt JS (1998) Cerebral blood flow increases over the
607 first three days of life in extremely preterm neonates. Arch Dis Child - Fetal Neonatal
608 Ed 78:F33–F37.
609 Molavi B, Dumont GA (2012) Wavelet-based motion artifact removal for functional near-
610 infrared spectroscopy. Physiol Meas 33:259–270.
611 Penfield W, Boldrey E (1937) SOMATIC MOTOR AND SENSORY REPRESENTATION IN
612 THE CEREBRAL CORTEX OF MAN AS STUDIED BY ELECTRICAL
613 STIMULATION. Brain 60:389–443.
614 Pryds O, Greisen G (1989) Effect of PaCO2 and Haemoglobin Concentration on Day to Day
615 Variation of CBF in Preterm Neonates. Acta Paediatr 78:33–36.
616 Quast KB, Ung K, Froudarakis E, Huang L, Herman I, Addison AP, Ortiz-Guzman J,
617 Cordiner K, Saggau P, Tolias AS, Arenkiel BR (2017) Developmental broadening of
618 inhibitory sensory maps. Nat Neurosci 20:189–199.
619 Ranger M, Grunau RE (2014) Early repetitive pain in preterm infants in relation to the
620 developing brain. Pain Manag 4:57–67.
621 Schouenborg J (2008) Action-based sensory encoding in spinal sensorimotor circuits. Brain
622 Res Rev 57:111–117.
623 Schweiger M, Arridge SR (2014) The Toast++ software suite for forward and inverse
624 modeling in optical tomography. J Biomed Opt 19:040801.
625 Seelke AMH, Dooley JC, Krubitzer LA (2012) The Emergence of Somatotopic Maps of the
626 Body in S1 in Rats: The Correspondence Between Functional and Anatomical
627 Organization. PLOS ONE 7:e32322.
628 Slater R, Cantarella A, Gallella S, Worley A, Boyd S, Meek J, Fitzgerald M (2006) Cortical
629 Pain Responses in Human Infants. J Neurosci 26:3662–3666.
630 Slater R, Worley A, Fabrizi L, Roberts S, Meek J, Boyd S, Fitzgerald M (2010) Evoked
631 potentials generated by noxious stimulation in the human infant brain. Eur J Pain
632 Lond Engl 14:321–326.
633 Tachtsidis I, Scholkmann F (2016) False positives and false negatives in functional near-
634 infrared spectroscopy: issues, challenges, and the way forward. Neurophotonics
635 3:031405.
636 Takano T, Tian G-F, Peng W, Lou N, Libionka W, Han X, Nedergaard M (2006) Astrocyte-
637 mediated control of cerebral blood flow. Nat Neurosci 9:260–267.
638 Theiler J, Eubank S, Longtin A, Galdrikian B, Doyne Farmer J (1992) Testing for nonlinearity
639 in time series: the method of surrogate data. Phys Nonlinear Phenom 58:77–94.

Thivierge J-P, Marcus GF (2007) The topographic brain: from neural connectivity to cognition. Trends Neurosci 30:251–259.

Treede RD, Kenshalo DR, Gracely RH, Jones AK (1999) The cortical representation of pain. Pain 79:105–111.

Verriotis M, Chang P, Fitzgerald M, Fabrizi L (2016a) The development of the nociceptive brain. Neuroscience 338:207–219.

Verriotis M, Fabrizi L, Lee A, Cooper RJ, Fitzgerald M, Meek J (2016b) Mapping Cortical Responses to Somatosensory Stimuli in Human Infants with Simultaneous Near-Infrared Spectroscopy and Event-Related Potential Recording. eNeuro 3:ENEURO.0026-16.2016.

Waldenström A, Thelin J, Thimansson E, Levinsson A, Schouenborg J (2003) Developmental learning in a pain-related system: evidence for a cross-modality mechanism. J Neurosci Off J Soc Neurosci 23:7719–7725.

Whitehead K, Laudiano-Dray P, Pressler RM, Meek J, Fabrizi L (2018) T152. Somatosensory evoked delta brush activity in very pre-term infants. Clin Neurophysiol 129:e60–e61.

Whitehead K, Papadelis C, Laudiano-Dray MP, Meek J, Fabrizi L (2019) The emergence of hierarchical somatosensory processing in late prematurity. Cereb Cortex 29:2245–2260.

Willoughby WR, Thoenes K, Bolding M (2020) Somatotopic Arrangement of the Human Primary Somatosensory Cortex Derived From Functional Magnetic Resonance Imaging. Front Neurosci 14:598482.

Worley A, Fabrizi L, Boyd S, Slater R (2012) Multi-modal pain measurements in infants. J Neurosci Methods 205:252–257.

Wyatt JS, Cope M, Delpy DT, Zee P van der, Arridge S, Edwards AD, Reynolds EOR (1990) Measurement of Optical Path Length for Cerebral Near-Infrared Spectroscopy in Newborn Infants. Dev Neurosci 12:140–144.

Supplements and Source Data

Figure 1 – Source Data 1. Significant concentration changes at each channel following innocuous mechanical stimulation (touch) of the heel and the hand and following heel lance *Minimum and maximum Δ[HbO] and Δ[Hb] at every channel and the corresponding latency. The range of Bonferroni-corrected p values across all significant timepoints is provided. ↓ = significant decrease only, ↑ significant increase only, ↑/↓ = both a significant increase and decrease were observed at different latencies. The location of each channel is shown in Figure 4.*

Stimulus	Channel	Max Δ[HbO] µM	Min Δ[HbO] µM	Direction of sig. Δ	p value	Max Δ[Hb] µM	Min Δ[Hb] µM	Direction of sig. Δ	p value
Lance	1	0.14 (6.8s)	-0.79 (15.9s)	↓	<.001 - .012	0.05 (0.1s)	-0.38 (7.1s)		ns
	2	-0.01 (8.2s)	-0.97 (22.7s)	↓	<.001 - .010	0.27 (22.9s)	-0.42 (8.2s)	↓	<.001 - .026
	3	0.03 (1.9s)	-0.61 (20.5s)	↓	<.001 - .014	0.03 (23.1s)	-1.03 (9.1s)	↓	<.001 - .012
	4	0.10 (8.9s)	-0.86 (23s)	↓	<.001 - .012	0.09 (22.6s)	-0.67 (8.3s)	↓	<.001 - .011

	5	0.24 (5s)	-0.67 (19.9s)	↓	<.001 - .016	0.62 (3.1s)	-0.12 (28.2s)	↑	<.001 - .007
	6	0.60 (12s)	-0.05 (2.1s)	↑	<.001 - .011	0.03 (18s)	-0.41 (7.3s)	↓	<.001 - .014
	7	0.53 (5.6s)	-0.20 (25.6s)	↑	<.001 - .018	0.00 (0.1s)	-0.99 (8.2s)	↓	<.001 - .016
	8	-0.18 (15.2s)	-0.62 (22.2s)	↓	<.001 - .012	0.39 (27.9s)	-0.47 (10.9s)	↑/↓	<.001 - .021
	9	0.31 (12.8s)	-0.58 (30s)	↓	<.001 - .013	0.68 (4.4s)	-0.13 (18.5s)	↑	<.001 - .013
	10	0.31 (7.2s)	-0.36 (16.4s)		ns	0.62 (2.9s)	-0.02 (26.3s)	↑	<.001 - .033
	11	0.94 (14.4s)	-0.11 (2.7s)	↑	<.001 - .018	0.13 (22.9s)	-0.35 (11s)	↓	<.001 - .021
	12	0.62 (8.2s)	-0.25 (29.6s)	↑	<.001 - .018	0.04 (17.8s)	-0.61 (11.3s)	↓	<.001 - .011
	13	0.96 (14.5s)	-0.45 (28s)	↑	<.001 - .012	0.01 (30s)	-0.56 (9.7s)	↓	<.001 - .057
	14	0.71 (15.7s)	0.02 (2.6s)	↑	<.001 - .016	0.00 (30s)	-0.39 (13s)	↓	<.001 - .022
	15	0.46 (17s)	0.10 (0.1s)		ns	0.72 (20.7s)	0.12 (0.9s)	↑	<.001 - .010
	16	0.91 (14.1s)	-0.39 (29.3s)	↑	<.001 - .010	0.44 (5s)	-0.12 (12.2s)	↑	<.001 - .012
	17	0.52 (12.1s)	-0.19 (24.3s)	↑	<.001 - .011	0.28 (23.6s)	-0.12 (14.2s)	↑	<.001 - .025
Foot touch	1	0.04 (6.9s)	-0.25 (30s)	↓	<.001 - .018	0.09 (19.1s)	-0.08 (9.5s)	↑/↓	<.001 - .022
	2	0.09 (20.2s)	-0.09 (30s)		ns	0.09 (30s)	-0.03 (8.3s)	↑	<.001 - .014
	3	0.07 (2.7s)	-0.12 (25.2s)		ns	0.07 (4s)	-0.2 (11.2s)	↓	<.001 - .014
	4	0.00 (12.6s)	-0.11 (24.1s)	↓	<.001 - .013	0.03 (30s)	-0.13 (11.2s)	↓	<.001 - .012
	5	0.07 (11s)	-0.06 (30s)		ns	0.03 (30s)	-0.04 (13.1s)		ns
	6	0.09 (9.1s)	-0.05 (28.2s)		ns	0.03 (3.1s)	-0.1 (11.2s)	↓	<.001 - .030
	7	0.03 (0.9s)	-0.11 (18.5s)		ns	0.01 (5s)	-0.13 (11.4s)	↓	<.001 - .016
	8	0.19 (14.5s)	-0.05 (24.2s)	↑	<.001 - .010	0.05 (4s)	-0.1 (10s)		ns
	9	0.21 (9.3s)	-0.04 (26.1s)	↑	<.001 - .011	0.09 (24.5s)	-0.11 (12.4s)		ns
	10	0.04 (10.4s)	-0.10 (28.7s)		ns	0.09 (28s)	-0.06 (12.8s)	↑	<.001 - .013
	11	0.03 (17.4s)	-0.07 (24.7s)		ns	0.11 (24.6s)	-0.07 (11.3s)	↑	<.001 - .018
	12	0.16 (14.4s)	0.02 (5.2s)	↑	<.001 - .026	0.05 (5.4s)	-0.08 (30s)	↑/↓	<.001 - .016
	13	0.09 (13.4s)	-0.06 (5.6s)		ns	0.07 (4.5s)	-0.1 (15.8s)	↑/↓	<.001 - .013

	14	0.27 (14.7s)	0.00 (30s)	↑	<.001 - .018	0.10 (4.2s)	-0.1 (27.4s)	↑/↓	<.001 - .055
	15	0.07 (11.8s)	-0.09 (26.8s)		ns	0.02 (4.6s)	-0.16 (11.4s)	↓	<.001 - .011
	16	0.30 (15.8s)	0.03 (0.1s)	↑	<.001 - .029	0.10 (15.8s)	-0.05 (29.6s)	↑	<.001 - .014
	17	0.13 (17s)	-0.13 (30s)	↑	<.001 - .012	0.08 (19.7s)	-0.09 (9.4s)	↑/↓	<.001 - .049
	1	0.25 (11.3s)	-0.05 (23.5s)	↑	<.001 - .022	0.02 (29.9s)	-0.09 (3.4s)		ns
	2	0.28 (17.3s)	0.02 (1.4s)	↑	<.001 - .011	0.03 (30s)	-0.14 (9s)	↓	<.001 - .017
	3	0.31 (16.9s)	-0.10 (1.1s)	↑	<.001 - .035	0.04 (1.2s)	-0.16 (17s)		ns
	4	0.21 (19.1s)	-0.05 (6.4s)	↑	<.001 - .015	0.02 (7.2s)	-0.21 (17.7s)	↓	<.001 - .013
	5	0.12 (8s)	-0.07 (14.7s)		ns	0.05 (23.1s)	-0.05 (28.3s)		ns
	6	0.19 (21.5s)	-0.07 (1.4s)	↑	<.001 - .015	0.03 (30s)	-0.14 (13.1s)	↓	<.001 - .012
	7	0.07 (1s)	-0.12 (23s)		ns	0.12 (29.5s)	-0.07 (0.9s)		ns
	8	0.17 (11.4s)	-0.05 (24.1s)		ns	0.03 (24s)	-0.17 (17.6s)	↓	<.001 - .019
Hand touch	9	0.05 (0.2s)	-0.21 (28.9s)	↓	<.001 - .013	0.13 (24s)	-0.09 (2.6s)		ns
	10	0.06 (15.8s)	-0.15 (7.7s)		ns	0.04 (20.3s)	-0.07 (15s)		ns
	11	0.08 (5.2s)	-0.25 (20.5s)	↓	<.001 - .013	0.09 (22.9s)	-0.15 (9.6s)	↓	<.001 - .011
	12	0.09 (3.1s)	-0.15 (23.8s)	↓	<.001 - .011	0.11 (30s)	-0.09 (8.7s)	↑	<.001 - .011
	13	0.09 (3s)	-0.27 (20.3s)	↓	<.001 - .012	0.05 (28s)	-0.12 (9s)	↑/↓	<.001 - .013
	14	0.10 (3.2s)	-0.14 (23.3s)		ns	0.01 (22.7s)	-0.12 (6.2s)	↓	<.001 - .010
	15	0.11 (2.4s)	-0.15 (16.7s)	↓	<.001 - .010	0.13 (24.7s)	-0.01 (1.3s)	↑	<.001 - .038
	16	0.07 (1.3s)	-0.09 (8.6s)		ns	-0.02 (5.4s)	-0.08 (16.1s)	↓	<.001 - .015
	17	0.13 (27.2s)	-0.04 (17s)		ns	0.04 (23.8s)	-0.04 (6.3s)		ns

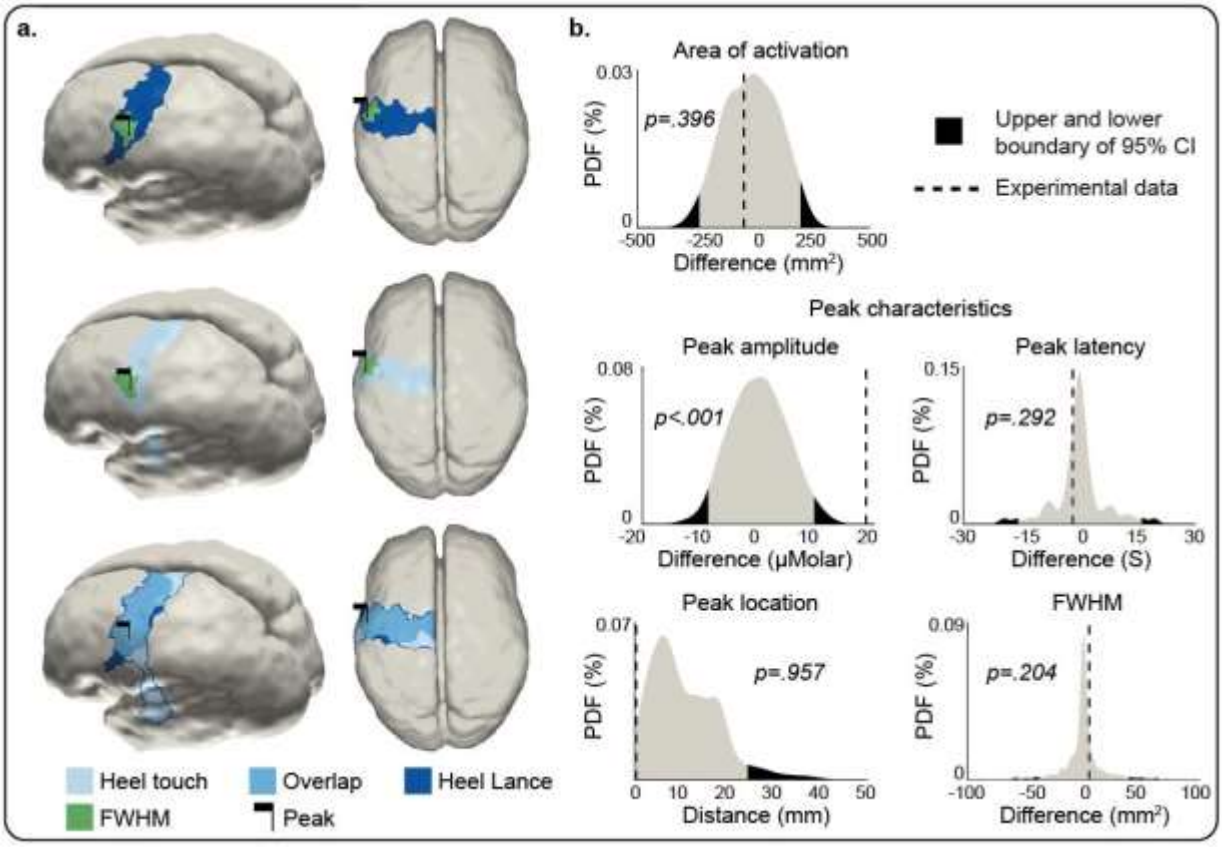

Figure 3 – figure supplement 1.

Average Δ[Hb] during a heel lance and innocuous mechanical stimulation (touch) of the heel and comparison of the peak change. *Left (a): Average Δ[Hb] following a heel lance and innocuous mechanical heel stimulation at the peak latency; Dark blue (lance) and pale blue (touch) patches represent the cluster of neighbouring nodes which are significantly larger (HbO) than baseline and mid blue is the area of overlap. Green patches represent the full width half maximum (FWHM) within these clusters. Black flags denote the location of the peak change. Right (b): Null distribution of the differences between amplitude, latency, location, and spread of the peak change, obtained with bootstrapping and phase scrambling (1000 iterations). Black shaded areas represent the 2.5 and 97.5 (or 95 for location) percentile of the distribution and black dashed lines represent the values obtained with the experimental data.*

The equivalent plots for Δ[Hb] are shown in Figure 3 – figure supplement 1 and Figure 3 – source data 1.

Figure 3 – Source Data 1. Comparison of Δ[HbO] and Δ[Hb] between heel lance and heel touch

Parameter estimates for the Δ[HbO] and Δ[Hb] following a heel lance and heel touch, and p value from statistical comparison. The Euclidean distance between the heel touch and heel lance peak locations has been provided rather than x,y,z coordinates of each peak. Linked to Figure 3 and Supplementary Figure 1.

	Δ[HbO]			Δ[Hb]		
Parameter	**Lance**	**Heel touch**	**p value**	**Lance**	**Heel touch**	**p value**
Overall spread (mm²)	396.18	235.11	.088	287.93	329.46	.396
Peak amplitude (μM)	15.23	4.13	.007	22.87	4.34	<.001
Peak latency (s)	14.1	15.8	.356	9.6	11.3	.292

Peak location (mm)	Euclidean distance = 1.63		.776	Euclidean distance = 0		.959
Peak spread (mm²)	66.63	52.96	.015	87.86	83.1	.204

705
706